SIMULATIONS AND EXPERIMENTS OF THE SEEDBED STRAW AND SOIL DISTURBANCE AS AFFECTED BY THE STRIP-TILLAGE OF ROWCLEANER (DEM)
/
带状耕作对种床秸秆清除率和土壤扰动的仿真与试验

Weiwei WANG, Jiale SONG, Guoan ZHOU, Beituo PAN, Qingqing WANG, Liqing CHEN *)

1) College of Engineering, Anhui Agricultural University, Hefei 230036, China
2) Laboratory of Engineering of Agricultural Machinery Equipment of Anhui Province, Hefei 230036, China

Keywords: *biomimetic; vertical rotary tillage; row clean; anti-blocking*

ABSTRACT

Strip-tillage is an effective option for proper seedbed preparation because it ensures the suitable conditions for seed germination and has been widely implemented. This study developed a strip-tillage of corn planter row cleaner using bionic vertical rotary blades to remove seedbed straw and ideal soil for no tillage sowing can be created. Through the qualitative analysis of the serrated arrangement contour of the praying mantis foreleg tip, the characteristic curve of the praying mantis foreleg tip was extracted and fitted, and the bionic geometric structure surface of the vertical rotary blade was constructed. The model and interaction system were established in EDEM 2.6 simulation environment, and their physical properties were calibrated with the real properties of lime concretion black soil and wheat straw. According to theoretical design to set simulation parameters, the radius of the cutter head was set to 120 mm, the driving speed of the cutter shaft was set to 500 r/min, and the depth of the cutting edge was set to 10 mm, the operating velocity of the active anti-blocking device was set to 5 km/h. The experiment results show that when the moving speed ratio is increased from 2.8 to 4.5, compared with the traditional vertical rotary blades, the straw removal rate and soil uniformity of seed bed are increased by 6.4% and 9.3%, and the average torque of the rotary tiller has been reduced by 12.3% respectively, the process effect and sowing quality being effectively improved. The study can provide theoretical reference for realization of no-tillage sowing vertical rotary tillage blade to reduce resistance and consumption and improve the quality.

摘要

带状耕作是可以为种子发芽提供良好环境的一种途径，已经被广泛应用。本文设计了一种基于螳螂趾多段锯齿状结构的立式仿生清茬防堵装置。通过对螳螂前肢尖锯齿状排列轮廓进行了定性分析，提取并拟合出螳螂前肢尖特征曲线，构建了立式旋耕刀的仿生几何结构曲面。运用 EDEM 软件构建无支撑秸秆全覆盖土壤离散元模型，在秸秆-土壤-仿生立式清茬防堵装置系统中进行秸秆移位虚拟仿真，设了仿生立式清茬防堵装置的刀轴驱动转速为500r/min、回转半径为 150 mm 及刀齿入土深度为10mm，利用仿真数据对秸秆扰动位移、清秸率进行分析，检验仿生立式清茬防堵装置结构参数和运动参数设计的合理性，试验结果表明，当移动速度比由 2.8 提高到 4.5 时，与传统的立式旋耕刀相比，秸秆清理率和种床土壤均匀度分别提高了 6.4%和 9.3%，旋耕机的平均扭矩降低了 12.3%。本文的研究结果为实现免耕播种立式清茬防堵装置减少阻力和消耗，提高种床耕作质量提供了理论参考。

INTRODUCTION

No-till (less-till, direct-seeding) sowing is a kind of protective farming technical operation, which has the advantages of maintaining soil moisture and saving labor and cost than traditional farming *(Sale et al., 2015; Li et al., 2019)*. However, the return of large quantities of crop residues to farmland also exposes disadvantages, as other equipment components can block and interfere with the process flow. Many studies have shown that crop residues thrown on the soil surface represent one of the main sources of interference in ensuring the process of strip-tillage and direct drilling *(Dikgwatlhe et al., 2014; Li et al., 2016)*. Therefore, it is urgent to research on a new type strip-tillage technology, which includes the advantage of full rotary-tillage seeding inasmuch as narrow soil strips can be removed residue and tilled rather deeply, having sown seeds and fertilizers into the strips cleaning area of tilled soil, subsequent seeds can grow under optimal condition similar to those of the fully rotary tillage. Moreover, strip-tillage combines the advantage of direct drilling, which facilitates the reduction of soil degradation processes and nutrient leaching, increases soil biological activity,

improves composition, conserves water, etc. *(Licht et al. 2010; Bilen et al., 2010; Jia et al., 2019)*. Therefore, to achieve the balance between soil conservation and organic matter content, it is necessary to take appropriate straw returning management measures, improve soil fertility and promote sustainable grain production.
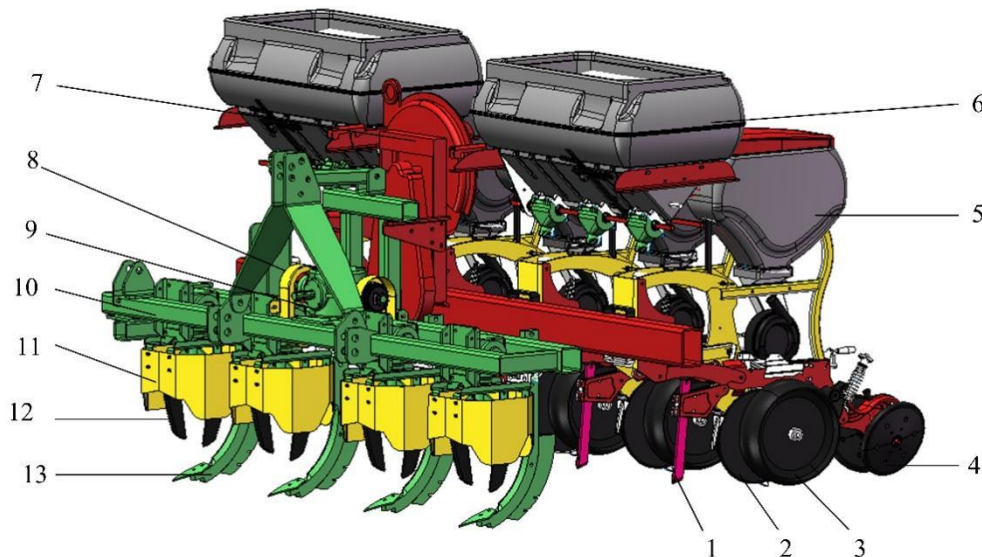
Row cleaner is a very important working part of no-tillage planter. It can ensure that all crop residues are removed from the soil strip, and do not mix the plant seeds into these residues, which prevent the good interaction between the seeds and soil, which has an adverse impact on seed germination *(Fallahi et al., 2008; Laufer et al., 2017)*. Compared with the soil part without seed metering device in direct drilling, the removal of crop residues from the soil part incorporated by plant seeds can improve the emergence rate and yield. In addition, removing crop residues from seed rows facilitates reducing the incidence of disease *(He et al., 2007)*. Many experts point out that the quantity of the previous crop left on the soil surface after harvest determines the operation quality of the no-till planter. The working quality of no-tillage planter is improved by adjusting the driving speed and working depth *(Celik et al., 2016; Vaitauskiene et al., 2017)*.

Wang et al, (2017), found that the traditional vertical rotary blade was used for cleaning the plant residues in the strip cultivation. Based on previous research, this paper combines the working principle of the no-tillage planter's straw removal, anti-blocking mechanism with the mantis toe characteristic and efficient cutting principle to design a bionic device that can realize the dual-cutter counter-rotating straw removal operation. Theory Analysis, test verification and other methods are used to clarify the influence of the operating parameters of the mechanism on the stubble removal and cutting performance so as to provide theoretical and technical support for the design of high-performance straw removal and anti-blocking devices.

MATERIALS AND METHODS
Structure and working principle

2BYQD-4A type active anti-blocking type corn no-tillage pneumatic planter is mainly composed of frame, suspension mechanism, row cleaners, layered fertilization device, wind pressure system, sowing device, ditching device, soil covering, pressing device and others, as shown in Fig.1. The technical parameters of corn no-tillage pneumatic planter are shown in Table 1.

Fig. 1 - Physical drawing of no-tillage air suction planter for corn
1- Opening share；2- Double disc trencher; 3- Earth covering device; 4- Depth limiting device; 5- Seed metering system;
6- Fertilizer discharge system; 7- Air pressure system; 8- Transmission case; 9- Chain power conveyor; 10- Frame;
11- Straw separator; 12- Row cleaner; 13- Layered fertilization subsoiler

Table 1

Main technical parameters of integration machine

Indexes	Parameters
Overall dimension (L×W×H) / (mm)	1960×2830×1620
Overall quality / kg	1000
Operation width / mm	1600-2800

Auxiliary power / kw	51.45-66.15
Speed of straw cleaner /（r/min)	450-600
Number of row cleaner	4
Straw cleaning radius / mm	15
Number of rows sown	4
Row spacing / mm	60
Sowing depth / mm	5-10
Depth of fertilization / mm	5-30
Theoretical plant spacing / mm	20-30
Operation speed / (m/s)	4-7

In this paper, the strip-tillage of row cleaner will be the research focus, which is mainly composed of double L-shaped rotary blades, rotary discs and bearings, which are vertically driven by the gearbox and commutator. The total length of the edge line of L-shaped rotary tiller is 200 mm and the length of soil cutting edge is 30mm, the radius of rotation is 150 mm, and the width of cutter head is 216 mm. According to the agronomic requirements of summer corn sowing, the sowing row spacing and depth were 400~600 mm and 30~50 mm, respectively. The lateral application of deep base fertilizer was generally applied to the sowing side 40~60 mm. The strip width of row cleaner was 240 mm, which was greater than the horizontal distance of the seed-fertilizer openers.

Feature extraction of mantis foot tooth contour curve

Many experts have carried out bionics research based on the peculiar physiological parts of animals (mole, locust, cricket, mole cricket), and designed a series of straw cutting parts and soil breaking parts of agricultural machinery with reference to the variable curvature contour characteristics of their toes, which effectively improves the straw breaking rate and reduces the cutting resistance *(Jia et al., 2018; Wang et al., 2019; Guo et al., 2017)*. As shown in Fig. 2, the leg and tibia of the mantis's forefoot are covered with hard and sharp serrations, which makes it have excellent predation ability. The unique physiological structure provides a reference for the design of soil crushing and straw breaking parts of agricultural machinery.

Fig. 2 - Tooth-shaped structure of mantis toes

Using MATLAB software in the rgb2gray, imerode, imdilate, im2bw, imfill, edge, bwperim function command in turn of the mantis front section photos on gray treatment, corrosion and expansion processing, binarization processing, hole filling, extract the boundary curves, the last frame expansion method is used to analyze the boundary curve connection, toes silhouette reconstructing CAD model, image after image processing using MATLAB software; the reconstructed model structure is clear, complete with the original sawtooth curves is shown in Fig. 3.
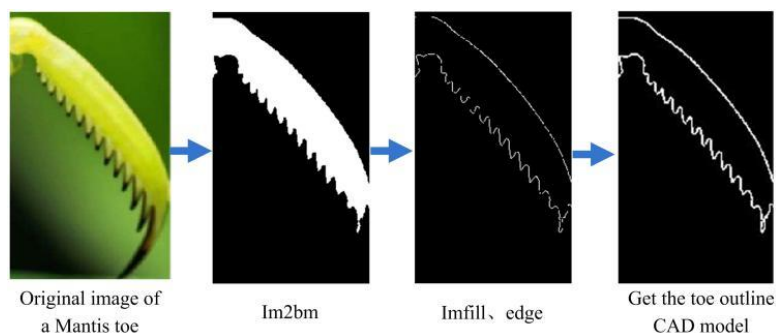

Fig. 3 - Extraction process of mantis toe curve

Extract the X and Y coordinates of the mantis toe model in the two-dimensional coordinate system, and fit a smooth serrated "edge" curve according to the coordinates of each point, as shown in Fig. 4. Due to the small cutting angle in the circle of the main cutting edge of the traditional vertical rotary tillage blade, the secondary cutting of soil and straw is formed when the rotary main cutting edge moves to the radian range [π, 2π], resulting in large resistance and increased vibration amplitude. However, too large internal cutting angle requires large blade width, which makes it difficult to balance the lateral force on the cutter head. At the same time, the straw is unsupported and irregularly sorted in the field, which will increase the difficulty of removing straw. The rotary operation process of the vertical rotary tillage knife should reduce the contact slip rate between the cutting edge and the straw layer to achieve rotary cutting and separation of straw, therefore the bionic vertical rotary tillage knife designed in this paper consists of a stubble breaking device, the increased serrations will make the longitudinal and horizontal straw not easy to slip from the cutting edge of the serrated blade, and at the same time increase the slip cutting effect between the blade and the straw, which can complete the rotary cutting of straw and separation of straw . The   sawtooth "cutting edge" curve was applied to the cutting edge of the vertical clear straw blade, and the particularity of the "cutting edge" curve of the mantis toes arrangement provided a basis for the cutting efficiency.
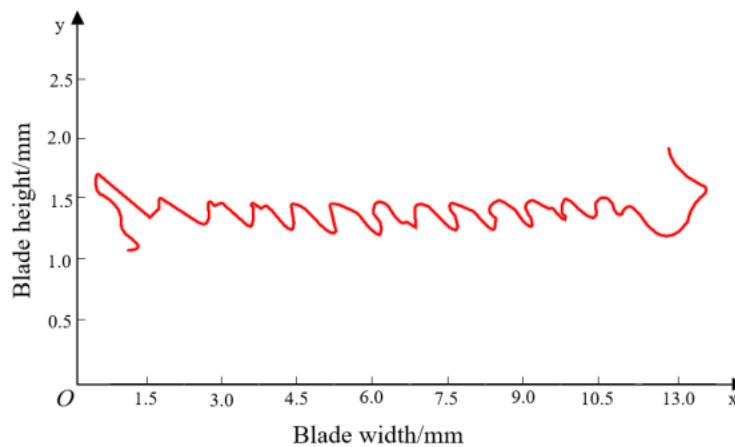

Fig. 4 - Sawtooth contour extraction and curve fitting

According to the fitted "cutting edge" curve and the idea of sawtooth for woodworking, the sharp "cutting edge" at the front end of tibia is selected as the sawtooth design model. The width of saw tooth is 1 ~ 1.5mm, the depth of saw tooth is 4.2mm, and the width of saw tooth bottom is 3.5 mm, because the sawtooth width and depth are too large in the actual operation process, it is easy to wind the straw, and too small causing severe wear and tear. The parameters of the bionic vertical rotary tillage blade were determined by repeated tests combined with the structural characteristics of the actual straw, as shown in Table 2. Its physical object is shown in Fig. 5.

Table 2

Mantis toes structure position

Name	X-axis coordinate position	Y-axis coordinate position
Convex starting point of first toe	2.78	1.46
Bottom of first toe	3.64	1.22
Convex starting point of second toe	3.75	1.42
Bottom of second toe	4.48	1.21
Convex starting point of third toe	4.45	1.42
Bottom of third toe	4.71	1.18
Convex starting point of fourth toe	5.25	1.45
Bottom of fourth toe	6.12	1.16
Convex starting point of fifth toe	6.14	1.43
Bottom of fifth toe	6.32	1.21

Fig. 5 - Sawtooth contour extraction and curve fitting

Movement analysis of bionic straw cutting device

Two bionic vertical rotary blades are installed and fixed on the cutter head in a dual way to form a straw breaking device. The center point O of the axis of the device makes a circular motion, and a fixed coordinate system is established with the rotation center of the straw breaking device as the origin. The positive direction of the X axis is consistent with the forward direction of the working planter, and the positive direction of the Y axis is vertical downward. Then, the trajectory equation of any point of the bionic straw breaking device is:

$$\begin{cases} x = R\cos \omega t + v_m t = R(\cos \alpha + \alpha/\lambda) \\ y = R\sin \omega t = R\sin \alpha \end{cases} \tag{1}$$

Where:

x and y are the position coordinates of the L-shaped blades at any point;

ω is the rotating angular velocity of the row cleaner;

φ is the rotation angle of the L-shaped blades;

v_d is the circumferential tangential velocity of point A;

v_m is operational speed of the planter forward direction;

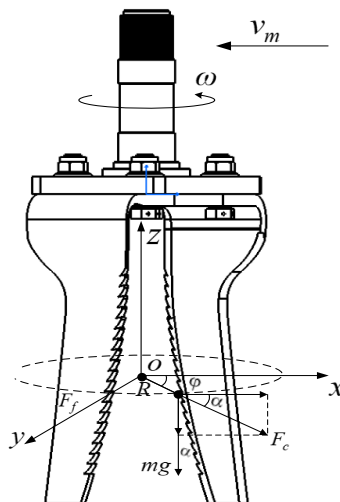λ is rotary tillage speed ratio, $\lambda = v_d/v_m$.

Fig. 6 - Cutting straw unit with the bionic rotary tillage blades

The movement track of the vertical rotary tillage blades is a trochoid, forcing the straw layer to circular flow in a strip. It was assumed that the flowing straw layer instantaneously subjected to the sliding cutting force *(Zhang et al., 2017)*. The flowing straw particles were thrown along the tangent direction at the linear velocity, when the sliding cutting force disappears. In order to obtain the critical condition that the straw-flow was thrown away from the row in the tangent direction of the blade trajectory, it was necessary to ensure that the tangent

direction component of rotary centrifugal force Fc was greater than the straw-flow unit by the soil layer rolling friction force. The force analysis of cutting straw layer trajectory was shown in Fig. 6. The rolling frictional force on the flowing straw particles was expressed as follows:

$$F_f = fmg + \frac{fmv_d^2 \sin\alpha}{R} \tag{2}$$

The condition under which the flowing straw layer can be centrifugally thrown to both sides of the seedbed is calculated using Eq. (3).

$$\frac{mv_d^2 \cos\alpha}{R} \geq fmg + \frac{fmv_d^2 \sin\alpha}{R} \tag{3}$$

Where:

m is the mass of flowing straw layer, [kg];

f is the friction coefficient between straw layer and soil layer;
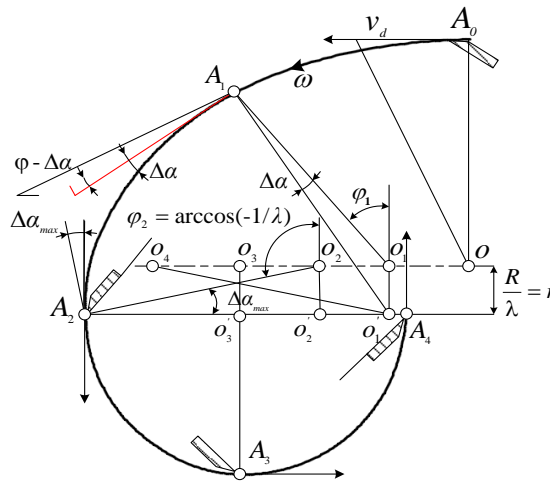
α is slide-cutting angle of the straight blades.

Fig. 7 - The moving trail of cutting edge at rotary tillage speed

When the rotation angle φ of the blades roll is from 0 to 2π (Fig. 7), as the tangential velocity decreases with increasing φ, the tangential velocity v_d at the point A_1 is calculated using Eq. (4):

$$v_d = \omega R \cos\Delta\alpha + \frac{\omega R}{\lambda} \cos(\phi - \Delta\alpha) \tag{4}$$

where $\Delta\alpha$ is the angle between the cutting velocity of point A and the peripheral velocity, the dynamic cutting angle $\Delta\alpha$ at points A_0 and A_3 approaches 0, respectively.

where the absolute velocity of point A_0 is the sum of the vector of circumferential velocity and forward velocity, the absolute velocity of point A_3 is the vector difference between them. Eq. (5) is obtained from Fig.7 as follows:

$$\frac{\omega R}{\sin(\varphi - \Delta\alpha)} = \frac{\omega R}{\lambda \sin(\Delta\alpha)} \tag{5}$$

Dynamic cutting angle calculated from Eq. (6)

$$\Delta\alpha = \text{arc tg} \frac{\sin\phi}{\lambda + \cos\phi} \tag{6}$$

Eq. (6) shows that the maximum value of dynamic slide-cutting angle depends on the slide-cutting angle of the straight blade, the rotary speed ratio λ of the row cleaner.

By formula (6) to solve the blade roller corner:

$$\varphi_2 = \arccos(-\frac{1}{\lambda}) \tag{7}$$

The maximum cutting angle can be obtained by the value of:

$$\Delta \alpha_{max} = arc\sin\frac{1}{\lambda} \tag{8}$$

Analysis of the relationship between $\Delta\alpha$ and $f(\lambda)$ type, combined with anti-blocking type corn no-tillage pneumatic planter field operations 4 to 7 km/h and bench test on the basis of qualitative straw transfer required cutting speed, the concluded reasonable value of speed ratio is 2.8 to 4.5.

Bench test

Test preparation and testing

The experiments were conducted using the laboratory soil bin facility (6 m length × 1 m width × 0.6 m height), and a custom-built experimental single row cleaner using double L-shaped rotary blades was shown in Fig. 8. The forward speed of the electric sliding track was adjustable from 0 to 3 m/s. The soil environment covered with wheat straws was manually prepared before the experiment. Each experiment ensures that the straw coverage, surface roughness, moisture content and compactness were consistent. Basic data on straw and soil displacement were obtained by tracer in Fig. 9, and straw and soil from cultivated soil strips were removed for future development of the model *(Liu et al., 2010)*. At the speed of 1.5 m/s, the ridge clearing machine was used to plough once.
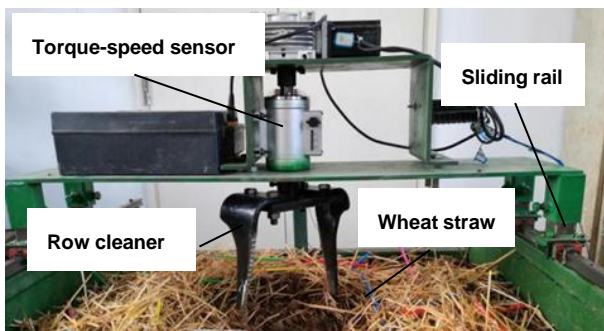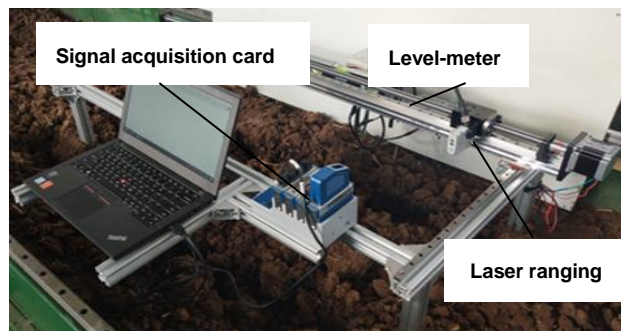

Fig. 8 - Soil and test

Fig. 9 - The soil surface measuring device

Evaluation indicators

(1) Straw removal rate

Straw removal rate refers to the percentage of straw removed in the total mass after seed metering device operation, a total of 20 groups of experiment data were collected. The effect of the technological parameters of the seed metering device on the distance between the straw and the center of the cultivated belt was studied. The actual straw amount was counted and weighed using the electronic balance in the straw cleaning area before and after the operation in the soil bin.

The arithmetic average values were m_1 and m_2, respectively. The straw removal rate is calculated as follows:

$$\eta = \left(1 - \frac{m_2}{m_1}\right) \times 100\% \tag{9}$$

Where:

η is straw removal rate, [%];

m_1 is the number of straw particles after simulation, [kg];

m_2 is the number of straw particles before simulation, [kg].

(2) Seedbed soil evenness

Seedbed soil evenness is a measure of the degree of soil concavity and convexity, and it plays an important role in mechanical sowing, irrigation and surface water accumulation, which directly affects the high and stable yield of crops and the water use efficiency of farmland. The soil surface micro-topography measuring device is a frame structure composed of aluminum profiles, as shown in Fig. 9. By measuring the spatial coordinates of the vertical axis, the device can determine the spatial position of the micro landform on the soil surface. According to the experimental method stipulated in GB/T 5668-2008 rotary tiller, the mean value of the standard deviation of the vertical axis height with m × n ranges was defined as the soil evenness of the tilled soil strip row, which was calculated as Eq. (10)

$$S_{mn} = \sqrt{\frac{\sum\limits_{j=1}^{m} \sum\limits_{i=1}^{n} (h_{i,j} - \bar{h})^2}{mn - 1}}$$ (10)

Where:

$h_{i,j}$ is vertical axis distance from arbitrary scanning point to datum level, mm;`

h is average vertical axis height of strip width, mm;

m is the number of forward scanning points in the measured area;

n is the number of lateral scanning points of the measured area;

S_{mn} is the soil evenness of the scanned area, mm.

RESULTS
Simulation analysis of bionic vertical rotary tillage blade
Simulation model building

In this paper, when using the discrete meta-analysis software EDEM to build the straw covering soil model, the parameters of the simulation model are shown in Table 3, following pre-tests and references to the literature *(Zhang et al., 2017)*, the working width of the simulation model of the cleaner unit is constructed according to the dimensions 3200mm×1000mm×400mm virtual soil bin covered with wheat straw. Set the soil thickness of the tillage layer to 250mm (321600 particles), the thickness of straw cover to 120 mm (11000 particles), and use layer-by-layer generation. Among them, in the process of soil particle generation, after free subsiding, it is loaded vertically above the soil particle group to ensure that the soil model is basically consistent with the actual tightness. The row cleaner model of the vertical rotary tillage device established by CATIA software was imported into EDEM, the tool was grounded at a depth of 10 mm, the speed was 500 r/min, the simulation fixed time step was 4.0×10^{-5}s, and Rayleigh time step was 25% and the total time was 3.5 s. The mesh unit is 3 times the minimum particle radius.
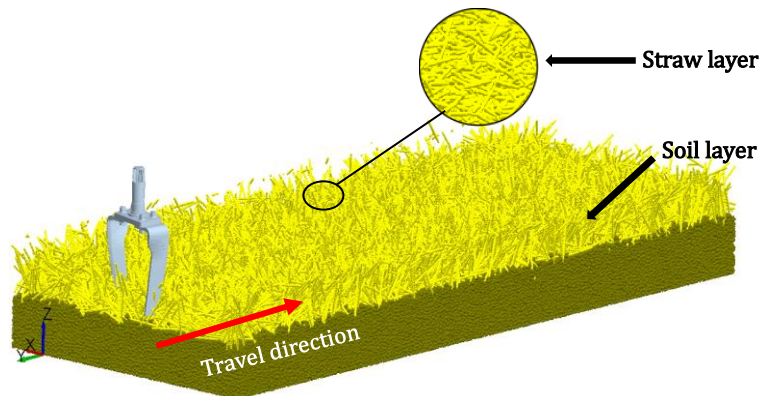

Fig. 10 - The straw-cleaner-soil model of with an enlarged image of straw clumps covered soil layers

Table 3

Calibration results of simulation experiment parameters

Parameters	Material			Parameters	Contact				
	Soil	Straw	Steel		Soil-Soil	Straw-Straw	Soil-Straw	Soil-Steel	Straw-Steel
Density, ρ /(kg·m⁻³)	1 850	30	7861	Restitution(e)	0.6	0.6	0.6	0.6	0.6
Poisson's ratio, v/m·s⁻¹	0.3	0.4	0.3	Static friction (f_s)	0.7	0.5	0.35	0.5	0.3
Shear modulus, G/Pa	$5×10^7$	$1×10^6$	$7.9×10^{10}$	Rolling friction (f_r)	0.225	0.01	0.015	0.05	0.01

Analysis of simulation results

Using the calibrated micro-parameters, the performance of the straw-cleaner-soil model was evaluated in terms of the straw displacement and cleaning rate. After the row-cleaner passage, the tangential force and displacement curves of each of the five straw tracers were plotted against the time. The straw moved laterally and forwardly when it was subjected to circumferential tangential force instantaneously. Fig. 11(a) shows that the average value of tangential force was 142 m·N, which decreased to 0 m·N with the friction resistance between the straw particles. *Zeng et al., (2020)* found that straw movement during tillage was modeled as three phases, namely forced, projectile, and overturning displacement, by means of video recording, mathematical modelling, and experimental validation. The moving trajectory of the five straw tracers shown nonlinear semi arc shape, which were away from a tilled soil strip row in Fig. 11(b).
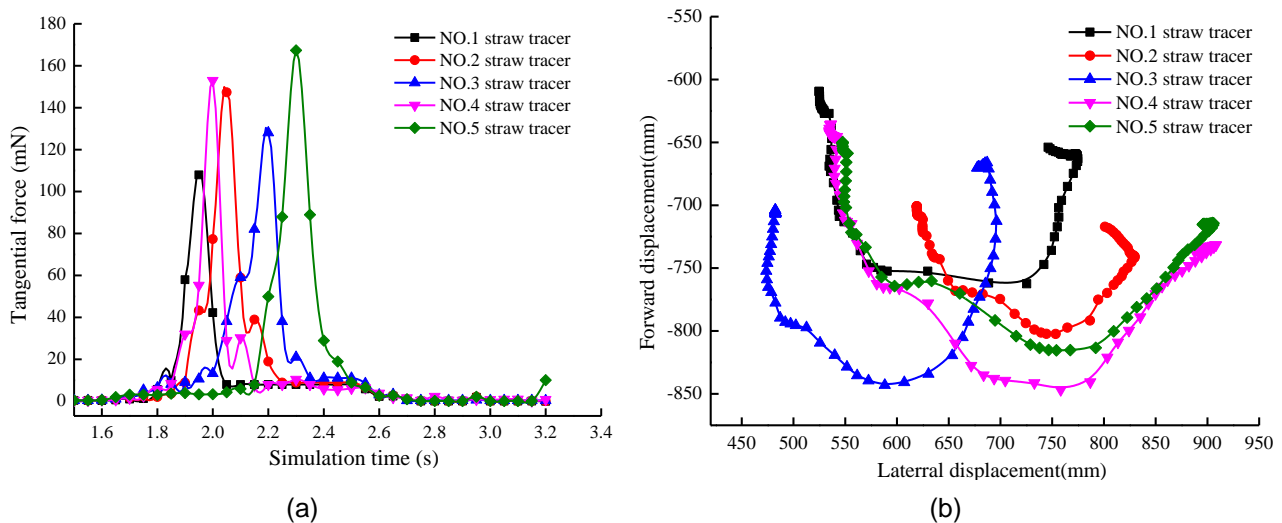

(a)   (b)

Fig. 11 -The force and displacement curve of five straw tracers

The length of straw and the mass of surface straws were 135 mm and 352 g·m⁻² respectively. The tillage speed of planter was 5 kw/h. Regardless of the situation that the straw particles were cut off, the position of the straw particle changed with the disturbance of the row cleaner during the simulation process. The simulation results showed that the covered straws were cleared from the travel path almost entirely on both sides of the seedbed, the straw displacement effect at different times are shown in Fig.12. The number of straw particles were statistically in the initial and ending positions of the simulated operation area, where the displacement of the straw particles was tracked, the average value of removal rate was 94.3% in the row sowing strip area.

From these simulation results, it can be clearly validated that using bionic vertical rotary tillage blades realized the anti-blocking idea of straws removal from a tilled soil strip row.
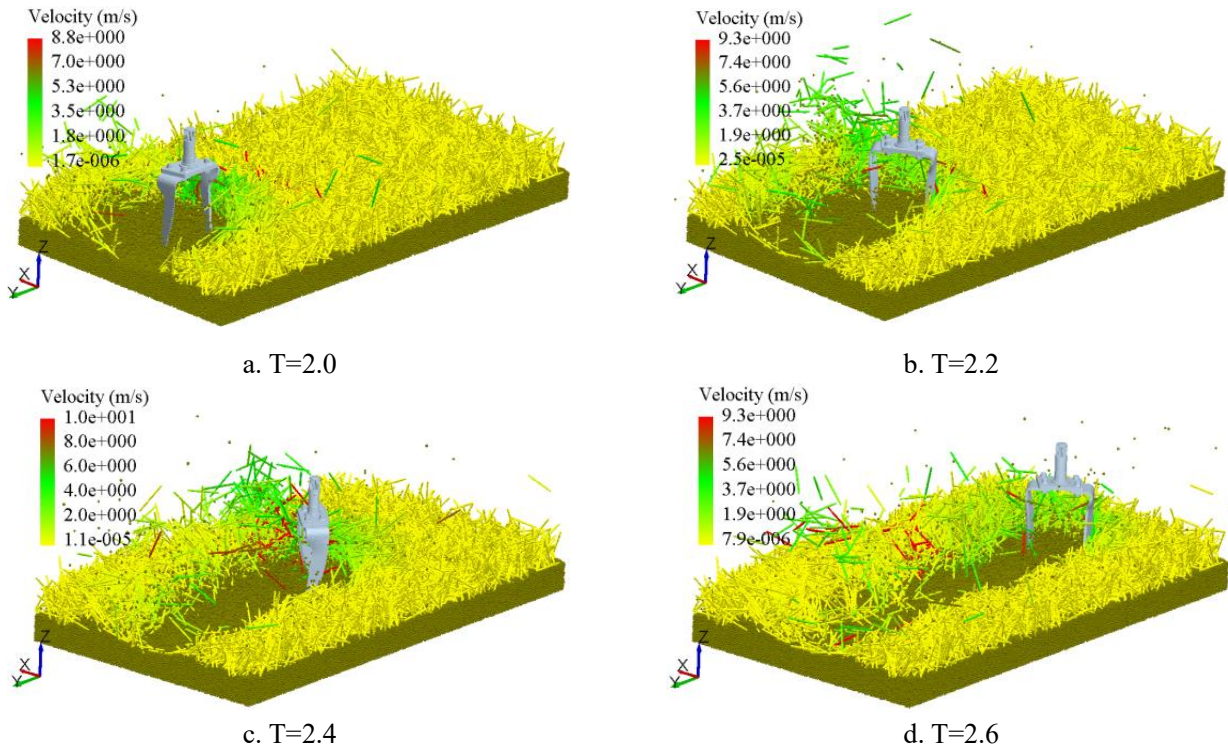
a. T=2.0

b. T=2.2

c. T=2.4

d. T=2.6

Fig. 12 - Straw displacement effect at different simulation times

Experiment results

The effects of rotation speed on straw removal rate and soil surface flatness were studied by bench test. According to the characteristics of wheat straw rhizome and theoretical consideration *(Zhou et al.,2020)*, the tillage depth of row cleaners in the range of 0~40 mm was selected as the controllable treatment factor, each factor being divided into five levels. In every trial, the length of the soil bin was separated into three parts, and randomly assigned 20 with the same straw coverage. The selection of evaluation index is the same as the simulation, in the course of bench test, the calculation of straw removal rate is the quality change within the width of tool work before and after the operation, and soil flatness is obtained by using the measurement system developed independently in the previous period *(Wang et al., 2019)*. Fig.13 showed straw removal rate and soil evenness after operation under different parameters.
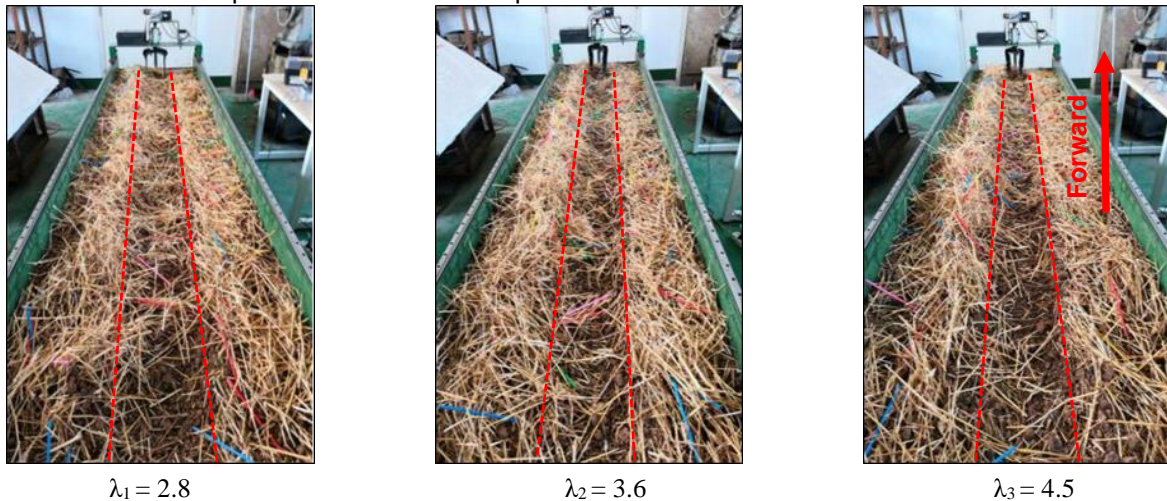

$\lambda_1 = 2.8$ $\lambda_2 = 3.6$ $\lambda_3 = 4.5$

Fig. 13 - Straw removal rate and soil evenness after operation under different parameters

All the obtained spatial coordinates of soil surface can be imported into the software MATLAB to generate the three-dimensional figure of soil surface in the sample. Fig.14 showed the surface microrelief of a tilled soil strip row under tillage depth of 20 mm in the soil bin. This indicates that a flat "U" type shallow furrow with a width of 240 mm was formed by bionic vertical rotary blades for strip-tillage, the values of soil evenness were calculated by Eq. 10, which was reduced from 25.3 mm to 8.5 mm before and after operation.

The three section profiles were randomly selected from a tilled soil strip row, Fig.15 showed that the bottom curve of groove profile fluctuates less, all groove contour curves coincide basically. From these results, when cutting seedbed using bionic vertical rotary blades, it can be clearly seen a flat "U" type shallow furrow to improve the stability of sowing depth.
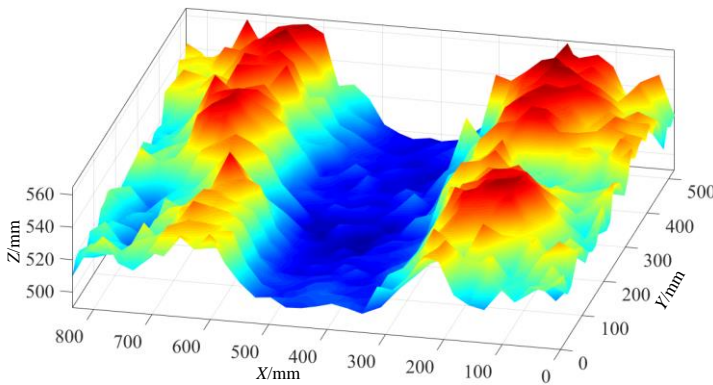
Fig. 14 - The flat "U" type shallow furrow with a width of 250 mm was formed after strip-tillage
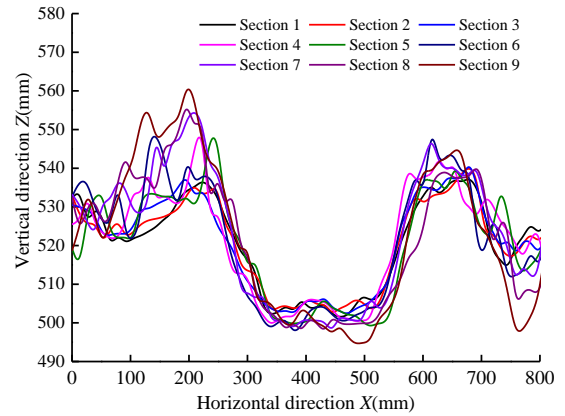
Fig. 15 - Groove section profile superposition curve from a tilled soil strip row

Fig.16 shows the measured values of straw cleaning rate and soil flatness under different motion speed ratios of three anti-blocking mechanisms during the experiment. The experimental results show that the straw cleaning rate increases with the increase of λ (the horizontal displacement and lateral displacement of straw increase), under the three speed ratios, the straw cleaning rate of the anti-blocking mechanism of the spiral sawtooth blade is higher than that of the traditional vertical straight blade and spiral blade, λ from 2.8 to 4.5, the straw removal rate in the operation area of the three anti blocking mechanisms increased by 8.3%, 6% and 4.8% respectively, and the difference among the three speed ratios was significant (P < 0.05); this is because the straw particles are in a discrete state, which is different from the volume of soil cutting block. When the motion speed ratio is 2.8, the horizontal displacement and transverse displacement of straw in the residual cycloid missed tillage area are relatively small, resulting in a large amount of straw residue in the strip tillage area.

As shown in Fig. 17, the soil flatness after three cutter operations under different speed ratios increases with the moving speed ratio λ the lower the flatness of the increased surface (the better the leveling effect), λ from 2.8 to 4.5, the surface roughness of the farming area decreased by 1.13mm, 0.46mm and 0.77mm respectively after the operation of the three anti blocking mechanisms, and the difference among the three motion speed ratios was significant (P < 0.01). Compared with the traditional vertical straight blade, soil uniformity of seed bed has been improved 9.3%.
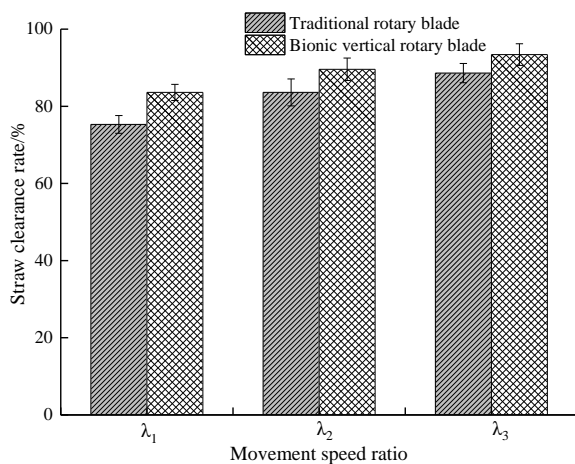
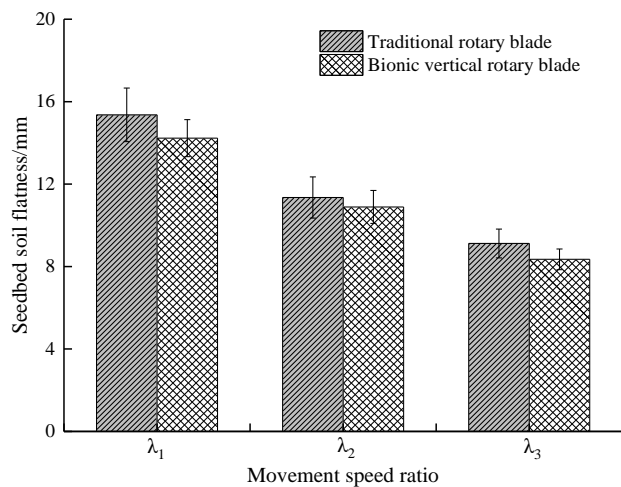**Fig. 16 - Straw removal rate under different speed ratios**

Fig. 17 - Soil flatness under different speed ratios

According to the power consumption comparison at different times in Fig.18, the torque of bionic vertical rotary blades under the same conditions is mostly lower than that of traditional vertical rotary blades, and the power consumption of bionic vertical rotary blades can be reduced by 12.3% compared to traditional vertical rotary blades by the average calculation.
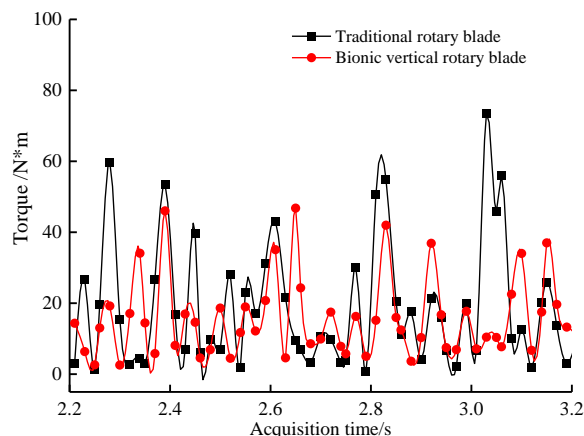
Fig. 18 - Comparison of power consumption at different acquisition times

CONCLUSIONS

The development of corn planter row cleaner using bionic vertical rotary tillage blades to remove seedbed straw and create ideal soil for no-tillage sowing, produce high-quality seedbeds for strip-tillage and production, so as to obtain the best seed germination and early seedling vigor. In this paper, an in-depth study of the rotation process of the bionic vertical rotating tillage blades has been carried out and compared with the rotation effect of conventional rotating blades through experimental verification. The specific conclusions were as follows:

In this study, the EDM simulations and experiments were used to collect and process the data, the hypothesis of the influence of some parameters on the straw removal rate and soil evenness was put forward, which was verified by simulations and bench experiment. Tillage speed have significant influence on the cutting process and results of straw and soil.

The experiments results showed that the straw removal rate of the anti-blocking mechanism of the spiral sawtooth blade is higher than that of the traditional vertical straight blade and spiral blade, the straw removal rate and soil level were improved by 6.4% and 9.3%, and the average torque of the rotary tiller has been reduced by 12.3%. Respectively, this design can provide reference for the design of no-tillage planter.

ACKNOWLEDGEMENT

REFERENCES

[1]   Bilen S., Celik A., Altikat S., (2010), Effects of strip and full–width tillage on soil carbon IV oxide–carbon (CO$_2$–C) fluxes and on bacterial and fungal populations in sunflower, *Afr. J. Bio technol*, 2010, 9 (38), 6312–6319.

[2]   Celik A., Altikat S., (2010), Effects of various strip widths and tractor forward speeds in strip tillage on soil physical properties and yield of corn, *J. Agric. Sci.*, 2010,16,169－179.

[3]   Dikgwatlhe S.B., Chen Z.D., Lal R., Zhang H.L., Chen F., (2014), Changes in soil organic carbon and nitrogen as affected by tillage and residue management under wheat-corn cropping system in the North China Plain, *Soil Tillage Res.* ,144, 110–118.

[4]   Fallahi S., Raoufat M.H., (2008), Row-crop planter attachments in a conservation tillage system: a comparative study, *Soil Tillage Res.*, 2008, 98, 27–34, https://doi.org/10.1016/j. still.2007.10.005.

[5] Guo J., Zhang Q.Y., Song J.N., et al., (2017), Design and experiment of bionic mole's toe arrangement serrated blade for soil-rototilling and straw-shattering, *Transactions of the Chinese Society of Agricultural Engineering (Transactions of the CSAE).*,33(6):43-50;

[6] He J., Li H.W., Wang X.Y., McHugh A. D., Li W. Y., Gao H.W., Kuhn N.J., (2007), The adoption of annual subsoiling as conservation tillage in dryland corn and wheat cultivation in northern China, *Soil Tillage Res.*, 2007,94, 493－502.

[7] Jia H.L., Guo M.Z., Guo C.J., et al., (2017), Design of Dynamic Bionic Straw Cutting Device and Optimization Test of Parameters, *Transactions of the Chinese Society for Agricultural Machinery.*, 49(10):103-114;

[8] Jia H. L., Wang Q., Huang D.Y., Zhu L. T., Li M. W., & Zhao, J.L. (2019), Design of bionic mole forelimb intelligent row cleaners, *Int J Agric & Biol Eng.*, 2019, 12(3), 27–35.

[9] Laufer D., Koch H.J., (2017), Growth and yield formation of sugar beet (Beta vulgaris L.) under strip tillage compared to full width tillage on silt loam soil in Central Europe, *Eur. J. Agric.*, 2017,82, 182–189. https://doi.org/10.1016/j.eja.2016.10.017.

[10] Li L.D., Wilson C.B., He H.B., Zhang X.D., Zhou F., Schaeffer S.M. (2 019), Physical, biochemical, and microbial controls on amino sugar accumulation in soils under long-term cover cropping and no-tillage farming, *Soil Biology & Biochemistry.*, 135, 369–378. https://doi.org/10.1016/j.soilbio.2019.05.017.

[11] Li S.Y., Gu X., Zhuang J. An T.T., Pei J.B., Xie H.T., Li H., Fu S.F., Wang J.K., (2016), Distribution and storage of crop residue carbon in aggregates and its contribution to organic carbon of soil with low fertility, *Soil Tillage Res.*,155, 199–206.

[12] Licht M.A., Al-Kaisi., (2010), Strip-tillage effect on seedbed soil temperature and other soil physical properties, *Soil Tillage Res.*, 80(1), 233–249.

[13] Liu J., Chen Y., & Kushwaha R. L., (2017), Effect of tillage speed and straw length on soil and straw movement by a sweep, *Soil Tillage Res*, 109, 9–17. https://doi.org/10. 1016/j.still.2010.03.014;

[14] Sale V., Aguilera P., Laczko E., Mäder P., Berner A., Zihlmann U., Marcel V.D.H., Oehl F., (2015), Impact of conservation tillage and organic farming on the diversity of arbuscular mycorrhizal fungi, *Soil Biology & Biochemistry.*, 84 ,38–52. http://dx.doi.org/10.1016/j.soilbio.2015.02.005.

[15] Vaitauskienė K., Šarauskis E., Romaneckas K., Jasinskas A., (2017), Design development and field evaluation of row-cleaners for strip tillage in conservation farming, *Soil Tillage Res*, 2017,174, 139–146. https://doi.org/10.1016/j.still.2017.07.006.

[16] Wang Q., Jia H.L, Zhu L.T, et al., (2017), Design and Experiment of Star-toothed Concave Disk Row Cleaners for No-till Planter, *Transactions of the Chinese Society for Agricultural Machinery.*, 50(2):68-77;

[17] Wang W.W., Li J., Wang Q.Q., et al., (2019), Chen L.Q. Design and Experiment for Tillage Soil Groove Measurement System, *Transactions of the Chinese Society for Agricultural Machinery*, 50(7):93-99;

[18] Wang W.W., Zhu C.X., Chen L.Q., et al., (2017), Design and experiment of active straw-removing anti-blocking device for maize no-tillage planter, *Transactions of the Chinese Society of Agricultural Engineering (Transactions of the CSAE).*, 33(24):10-17;

[19] Zeng Z. W., Chen Y., Zhang X. R., (2020), Modelling the interaction of a deep tillage tool with heterogeneous soil, *Computers and Electronics in Agriculture*, 2020,143, 130–138.

[20] Zhang X.R., Chen Y., (2017), Soil disturbance and cutting forces of four different sweeps for mechanical weeding, *Soil Tillage Res.*, 168, 167–175;

[21] Zhou H., Zhang C, L., Zhang, W, L., et al., (2020), Evaluation of straw spatial distribution after straw incorporation into soil for different tillage tools, *Soil Tillage Res.*, 196,104440. https://doi.org/10.1016/j.still.2019.104440;